

Thermal Conductivity of Ethane from 290 to 600 K at Pressures up to 700 bar, Including the Critical Region

R. C. Prasad¹ and J. E. S. Venart²

Received February 24, 1984

The paper presents thermal conductivity measurements of ethane over the temperature range of 290–600 K at pressures to 700 bar including the critical region with maximum uncertainty of 0.7 to 3% obtained with a transient line source instrument. A correlation of the data is presented and used to prepare tables of recommended values that are accurate to within 2.5% in the experimental range except near saturation, and in the critical region, where the anomalous thermal conductivity values are predicted to within 5%.

KEY WORDS: ethane; thermal conductivity; transport properties.

1. INTRODUCTION

Many measurement programs of the thermal conductivity of ethane (Table I) [1–14] have been reported. Only a few [4, 11, 12], however, cover extended temperature and pressure ranges. An earlier correlation attempt [15] emphasized the need for additional and more accurate measurements in a wider experimental range than had been obtained previously. In this paper, accurate measurements in the temperature range 295–600 K at pressures to 700 bar are presented. Measurements are also reported in the anomalous regions near the saturation line and the critical region. These data are correlated to within 2.5% in general and 5% in the anomalous region. The new correlation is used to prepare a thermal conductivity table for ethane.

¹ University of New Brunswick, Saint John, New Brunswick, Canada.

² University of New Brunswick, Fredericton, New Brunswick, Canada.

Table I. Thermal Conductivity of Ethane, Experimental

Ref. No.	Author(s)	Year	Temp. (K)	Pressure	Method	Uncertainty (%)	Remarks
1	Zeigler	1904	273.15	dilute gas	compensated hot wire		
1	Eucken	1913	273.15	dilute gas	compensated hot wire		
1	Moser	1929	273.15	dilute gas	compensated hot wire	0.2	
1	Mann, Dickins	1931	273.15	dilute gas	hot-wire	2.6	
2	Borovik et al.	1950	113-273	saturation pressure	concentric cylinder		
3	Senftleben, Gladish	1949	343.15	1 atm	concentric cylinder		
4	Lenoir et al.	1953	315-340	1-200 bar	concentric cylinder		
5	Senftleben	1953	303	dilute gas	hot-wire		99% pure sample
6	Vines, Bennett	1954	374, 399, and 422	dilute gas	compensated hot wire	1	
7	K.eyes	1954	325.05	0-39.4 atm	concentric cylinder		
			522.35	1 atm			
8	Lambert et al.	1955	339.15	dilute gas	compensated hot wire		
9	Leng, Comings	1957	341	1-261 atm	concentric cylinder		
10	Geier, Schäfer	1961	273-873	dilute gas	hot-wire	2	
11	Carmichael et al.	1963	277-444	1-340 atm	conductivity column	0.5	
12	Le Neindre et al.	1969	298-800	1-1200 bar	spherical shell	1.5	99.9% pure sample
13	Clifford et al.	1976	303	low pressure	concentric cylinder	0.7	99.87% pure sample
14	Yakush et al.	1979	318.8-590.2	dilute gas	hot-wire with thermistors	1	heated filament

2. EXPERIMENTAL PROCEDURE

The measurements were obtained with a transient hot-wire instrument that uses a $12.5\text{ }\mu\text{m}$ diameter platinum wire approximately 8 cm long. Various components of the apparatus, e.g., the conductivity cell, thermostat, pressurizing system, the measurement system, and the inherent errors and precision are described in detail elsewhere [16]. A summary of the technique of measurement will, however, be presented here to enable the reader to assess the experimental accuracy.

During an experiment, the platinum wire, immersed vertically in the test fluid, is heated electrically from zero time. To a first approximation, the wire behaves as an infinite line source of constant heat generation, and the conductivity is calculated from the temperature rise between times t_1 and t_2 according to the following equation [17]³:

$$\Delta T_w = \frac{Q_l}{4\pi\lambda} \ln(t_2/t_1) \quad (1)$$

The temperature-time transient of the wire is recorded with a computerized data-acquisition system. "Apparent" thermal conductivities at increasing time periods are computed by the data processing system, and a "true" conductivity is estimated by extrapolation to zero time with the condition [18]

$$\left. \frac{d\lambda}{dt} \right|_{t=0} = 0 \quad (2)$$

which ensures a zero-slope at $t = 0$. Corrections for the finite heat capacity of the wire and nonconstant heat dissipation are applied during data processing.

3. RESULTS

The thermal conductivity of ethane was measured along six nominal isotherms: 295, 318, 397, 498, and 600 K, at pressures to 700 bar. After careful selection on the basis of reproducibility and stability of experimental conditions, 239 measurements are reported (Appendix, Table AI). In addition to temperature (T , K), pressure (P , bar), and thermal conductivity (λ , $\text{mW} \cdot \text{m}^{-1} \cdot \text{K}^{-1}$), the fluid density (ρ , $\text{g} \cdot \text{cm}^{-3}$) is also tabulated. The accuracy and reproducibility of the apparatus were checked prior to as well as during these measurements and were estimated to be within 1.5 and 1%, respectively. The ethane sample was stated by the supplier (Matheson) to be 99.96% pure. IR and mass spectroscopic tests before and after the measurements indicated no change in the sample composition.

³ For an explanation of symbols, see nomenclature at end of article.

4. CORRELATION AND DISCUSSION

4.1. General Correlation

A correlation of the data was attempted according to a model (Fig. 1) suggested by Sengers et al. [19]:

$$\lambda(\rho, T) = \lambda_{bg}(\rho, T) + \Delta\lambda_{cr}(\rho, T) \quad (3)$$

$$\lambda_{bg}(T) = \lambda_1(T) + \Delta\lambda_e(\rho, T) \quad (4)$$

4.2. Thermal Conductivity at 1 Bar

The thermal conductivity of fluids is only temperature dependent [19–21] in the low density limit, and a correlation, proposed and used earlier [19], was employed:

$$\lambda_1(T) = \sqrt{T_r} \left/ \sum_{k=0}^n a_k/T_r^k \right., \quad T_r = T/T_{cr} \quad (5)$$

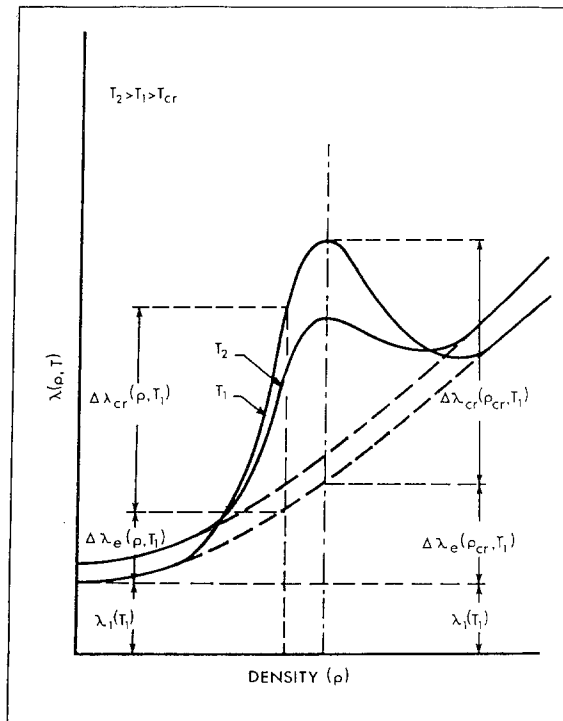


Fig. 1. The thermal conductivity model.

Table II. Thermal Conductivity of Ethane at 1 bar as a Function of Temperature

T (K)	$10^3\rho$ (g·cm $^{-3}$)	$\lambda_{1\text{ bar}}^a$ (mW·m $^{-1}\cdot\text{K}^{-1}$)	$\lambda_{\text{calc}, 1\text{ bar}}^b$ (mW·m $^{-1}\cdot\text{K}^{-1}$)	Deviation (%)
295	1.2540	20.28 ± 0.17	20.28	0
315	1.1720	22.97 ± 0.10	22.96	0.05
350	1.0528	27.94 ± 0.15	27.97	-0.11
400	0.9192	35.74 ± 0.19	35.80	-0.17
498	0.7371	53.53 ± 0.20	53.26	0.51
600	0.6113	73.91 ± 0.37	74.14	-0.31

^a Thermal conductivity values at 1 bar estimated by Eq. (6) in the low density region.^b Thermal conductivity values at 1 bar estimated by Eq. (5) with $n = 2$.**Table III.** Parameters of the Correlation Equations for the Thermal Conductivity of Ethane

- (a) Correlation for
- $\lambda_1(T)$
- in the range
- $295 \leq T \leq 600$
- K with Eq. (5):

$$\begin{aligned} n &= 2 & a_0 &= -0.284425 \times 10^{-3} \\ && a_1 &= 2.862191 \times 10^{-2} \\ && a_2 &= 1.786388 \times 10^{-2} \end{aligned}$$

- (b) Correlation for
- $A\lambda_e$
- as a function of density with Eq. (7):

$$\begin{aligned} b_0 &= 0.0 \\ b_1 &= 20.19189735 \\ b_2 &= 11.01952958 \\ b_3 &= 9.90113617 \end{aligned}$$

- (c) Correlation of
- $A\lambda_e$
- as a function of density and temperature
- $m = 2$
- ,
- $n = 3$
- , Eq. (8),
- b_{ij}

i	j	0	1	2	3
0	0.0	-14.158643	15.995975	1.917451	
1	-1.396130	62.824318	-54.924712	17.953475	
2	1.000647	-26.933607	27.389732	-9.696567	

- (d) Correlation of
- $A\lambda_{cr}$
- as a function of density and temperature with Eq. (9):

$$\begin{aligned} c_1 &= 0.40594041 \\ c_2 &= 0.01903895 \\ c_3 &= 0.14378686 \\ c_4 &= 1.86698399 \end{aligned}$$

The data at 1 bar were obtained by correlating the measurements at moderate densities for a particular isotherm with

$$\lambda = a_0 + a_1\rho + a_2\rho^2 + a_3\rho^3 + b(T - T_{av}) \quad (6)$$

The term $b(T - T_{av})$ was included to reduce the experimental data at T to the average temperature T_{av} [12]. A stepwise regression analysis of the data was performed to examine the necessity of the density terms ρ , ρ^2 , and ρ^3 in Eq. (6). Table II shows the thermal conductivity values (λ_1) estimated by this method at 1 bar in the range of 295–600 K.

A correlation of λ_1 within the experimental error was obtained with Eq. (5) for $n = 2$ (part a of Table III) using the critical parameters from ref. [22]. Figures 2 and 3 display the correlated values, the available experimental data, and a deviation plot.

4.3. The Excess Thermal Conductivity

The measurements in the high density regions indicated, in general, an increase in the excess thermal conductivity, $\Delta\lambda_e$, with density along any isotherm. Anomalous increases were observed in the critical region,

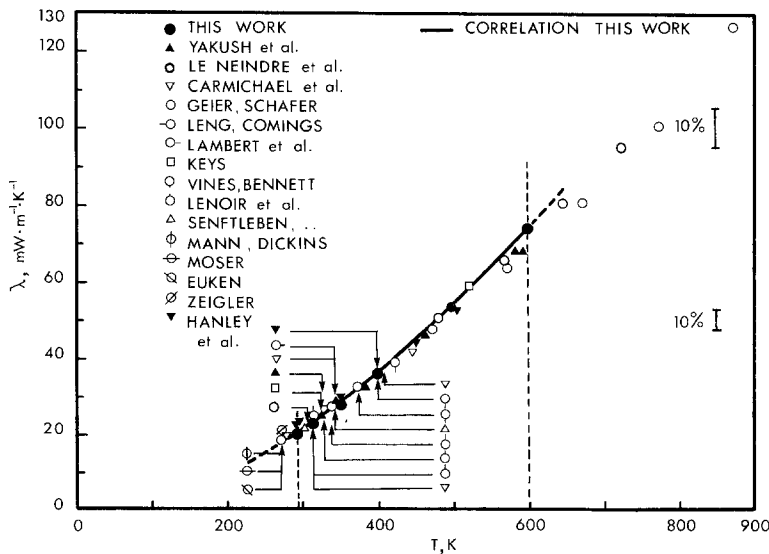


Fig. 2. Thermal conductivity of ethane at 1 bar: present correlation and values by other investigators. Values by Moser, Euken, and Zeigler are from Mann and Dickins [1]. Data by Senftleben are from refs. [3] and [5]. Data by Hanley et al [15] are from the errata cited.

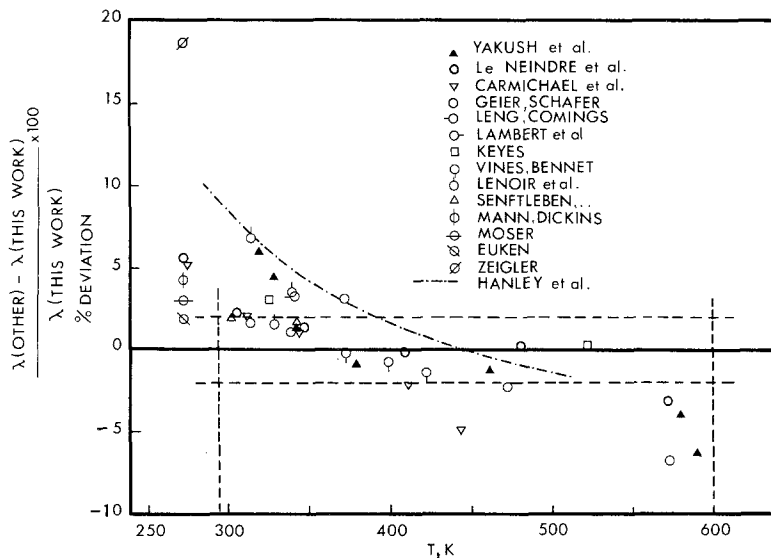


Fig. 3. Deviation plot: present correlation and data by other investigators for ethane at 1 bar. Values by Moser, Euken, and Zeigler are from Mann and Dickins [1]. Data by Senftleben are from refs. [3] and [5]. Data by Hanley et al [15] are from the errata cited.

particularly along the 318 K isotherm and near the liquid-vapor saturation lines at 295 K. This anomalous region is outlined in Table IV. Only data remote from the anomalous regions were used to develop a correlation.

The dependence of the excess thermal conductivity with respect to density alone was examined with

$$\Delta\lambda_e = \lambda(\rho, T) - \lambda_i(T) = \sum_{k=1}^n b_k \rho^k, \quad b_0 = 0 \quad (7)$$

Table IV. Density Range $\rho_{low} \leq \rho \leq \rho_{high}$ for Ethane as a Function of ΔT^* , Where Critical Enhancement in the Thermal Conductivity is Observed^a

T (K)	ΔT^*	ρ_{low} (g·cm ⁻³)	ρ_{high} (g·cm ⁻³)	$\Delta\rho_{low}^*$	$\Delta\rho_{high}^*$
295	-0.0338	0.05	0.42	-0.755	1.054
318	0.0317	0.05	0.40	-0.755	0.956
350	0.1463	0.06	0.38	-0.707	0.858
400	0.3101	0.12	0.30	-0.413	0.467
500	0.6376				
600	0.9651				

^a $\Delta\rho_{low}^* = (\rho_{low} - \rho_c)/\rho_c$; $\Delta\rho_{high}^* = (\rho_{high} - \rho_c)/\rho_c$.

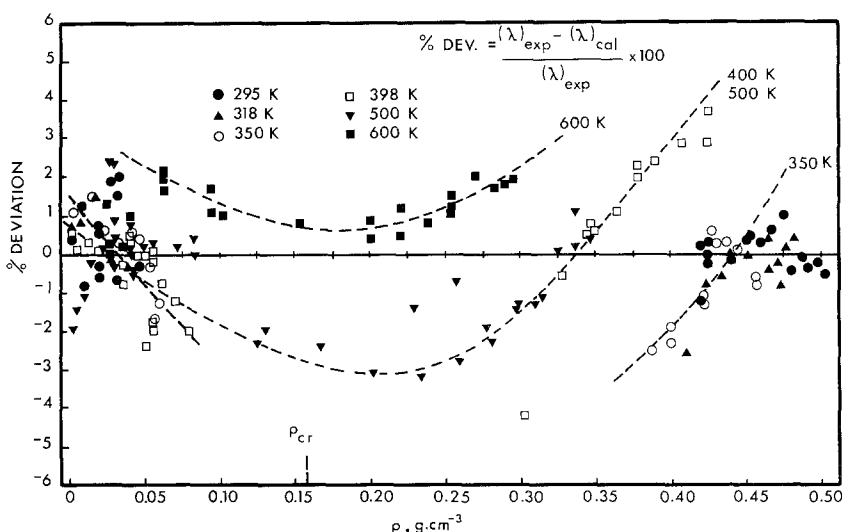


Fig. 4. Deviation plot: correlation of thermal conductivity of ethane from Eqs. (5) and (7).

On the basis of a stepwise regression procedure, the best three parameter model with $k = 1, 2, 3$ was selected and least squares estimates of b_k were obtained (part b of Table III). Figure 4 shows the deviation plot of all the experimental data used for this correlation. These deviations are of the same order as the experimental uncertainties. However, the nature of the deviations (Fig. 4) indicates a higher order temperature dependence.

A correlation in terms of density and temperature was next attempted with

$$\Delta\lambda_e(\rho, T) = \sum_{i=0}^m \sum_{j=0}^n b_{ij} T_r^i \rho_r^j, \quad b_{00} = 0 \quad (8)$$

and a representation within 2% was obtained with $m = 2$ and $n = 3$. The parameters b_{ij} are listed in part c of Table III, and the deviation plot is shown in Fig. 5. The qualitative as well as the quantitative improvement in the correlation is clearly demonstrated by Fig. 5 and Table V, respectively.

4.4. The Anomalous Thermal Conductivity

The anomalous conductivity value, $\Delta\lambda_{cr}$, was estimated by subtracting the background conductivity, $\Delta\lambda_{bg}$ (Eqs. 4, 5, and 8), from the experimental values in the region $-0.75 \leq \Delta\rho^* \leq 0.95$ and $\Delta T^* \leq 0.3$ (Table IV). A plot of $\Delta\lambda_{cr}$ versus ρ (Fig. 6) shows that the form of the anomaly is asymmetric

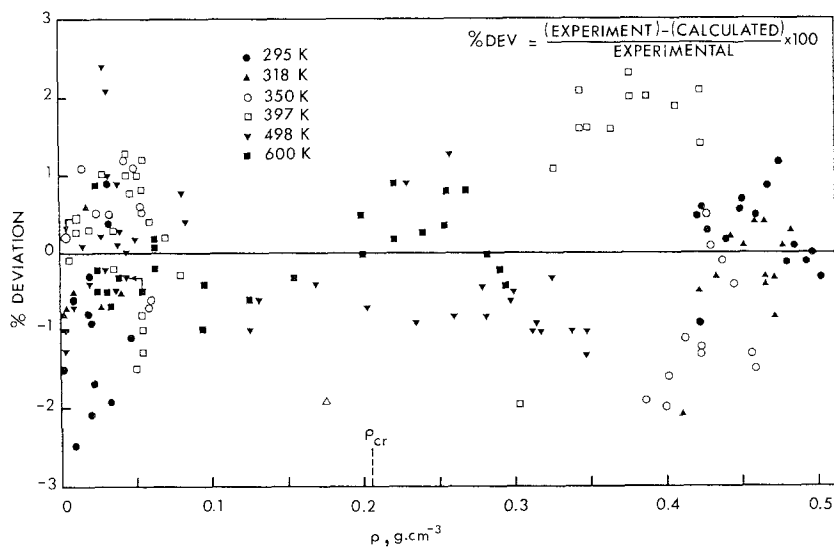


Fig. 5. Deviation plot: correlation of thermal conductivity of ethane from Eqs. (2) and (5).

about the critical density, with the maximum occurring at a density slightly higher than the critical density. These features are similar to those reported for other fluids [23, 24].

A correlation in terms of density and temperature was attempted in terms of

$$\Delta\lambda_{cr}(\rho, T) = Ae^{-x^2} \quad (9a)$$

with

$$A = \frac{c_1}{(\Delta T^*)^2 + c_2} \quad (9b)$$

$$x = c_4[\Delta\rho^* - c_3(\Delta T^*)^n] \quad (9c)$$

Table V. Comparison of Correlations with Eqs. (7) and (8)

Deviation	Magnitude	
	Eq. (7)	Eq. (8)
Maximum	$\pm 3\text{--}4\%$	$\pm 2\%$
Mean (absolute)	0.74	0.55
RMS (absolute)	1.07	0.77
Mean (%)	0.97	0.75
RMS (%)	1.28	0.96

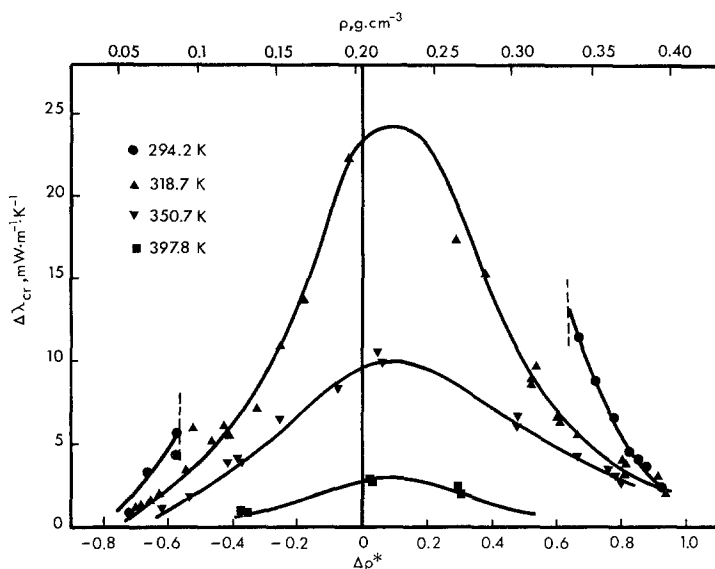


Fig. 6. Thermal conductivity enhancement for ethane, plot of $\Delta\lambda_{cr} \sim \Delta\rho^*$.

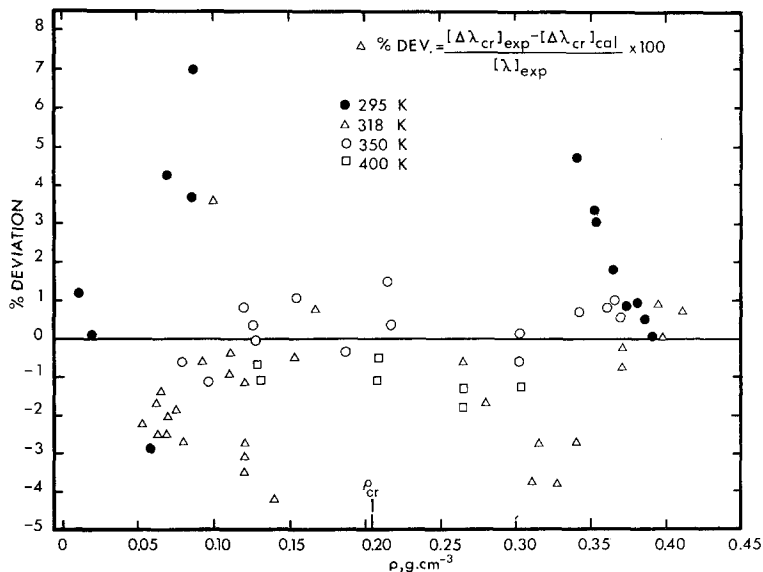


Fig. 7. Deviation plot: correlation of anomalous thermal conductivity, $\Delta\lambda_{cr}$, from Eq. (9).

This model is similar to that employed by Roder [25] with the exception that the expression for the amplitude term A , in Eq. (9b), has been modified to ensure maximum enhancement along the critical isotherm. Correlations within $\pm 5\%$ were obtained with $n = 0$ in Eq. (9c). The estimates of the parameters c_1 to c_4 are listed in part d of Table III, and the deviation plot is shown in Fig. 7.

5. COMPARISON AND DISCUSSION

The thermal conductivities estimated by the present correlation were compared with other experimental data in the temperature range of 290–600 K at 1 bar [1, 3–12, 14, 15] as well as over a range of pressures [4, 7, 9, 11, 12]. The deviation plots are shown in Fig. 2 and 8, respectively. Deviations in the anomalous region are also included in Fig. 8.

The majority of thermal conductivity values at 1 bar [3, 5–7, 12] are generally within $\pm 2.5\%$, while a few others [10, 11, 14] fall within about $\pm 5\%$ of the present correlation (Fig. 2). The experimental data of Le Neindre et al [12] show a reasonable agreement within about $\pm 5\%$ along five isotherms in the 310–570 K range. This data set contains some measurements in the anomalous region, where critical region enhancements of up to 19% are observed. These data are within 5% of those estimated by

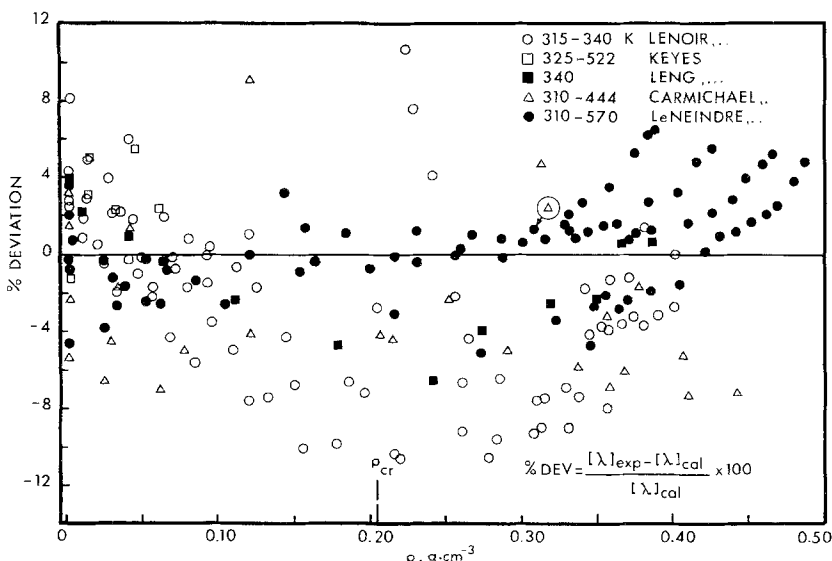


Fig. 8. Deviation of other experimental data from the present correlation, Eqs. (5), (8), and (9).

the present correlation. Some systematic deviation in the high density ($\rho > 0.3 \text{ g} \cdot \text{cm}^{-3}$) region is observed. The measurements of Leng and Comings [9] indicate an anomalous contribution of up to 16% along the 340 K isotherm and are within -6 to +4% of the new correlation. The few data reported by Keyes [7] show deviations between -1 to +5%.

Thermal conductivity data along three isotherms (315, 330, and 340 K) reported by Lenoir et al. [4] show critical region enhancements of about 60, 19, and 12%, respectively. These data show a maximum deviation of about 5%, except in the anomalous region, where the deviations increase to $\pm 10\%$. The data of Carmichael et al [11] do not show the anomalous effect in the density range indicated in Table IV along the 311 and 344 K isotherms. Only a single datum point at 311 K shows an enhancement of 33%, which agrees to within 9% of the present correlation. All other measurements are within -7 to +3% of the proposed correlation.

The present correlation has been developed on the basis of a correlation of experimental data obtained with a transient hot wire apparatus. These data have been shown to be accurate on the basis of a comprehensive error analysis [26]. The present correlation for the thermal conductivity anomaly is based on measurements in the extended critical region [25]. Thus the use of Eq. (9) is recommended only in that extended region. In the near-critical region specified by

$$|\Delta T^*| \leq 0.03 \quad \text{and} \quad |\Delta \rho^*| \leq 0.25 \quad (10)$$

the method recommended by Sengers et al. [19] should be employed.

6. CONCLUSIONS

The thermal conductivity of ethane has been measured in the range of 295–600 K at pressures to 700 bar and correlated to within $\pm 2.5\%$ in the experimental range except in the critical region. A model has been presented for the anomalous thermal conductivity in the extended critical region. It is felt that additional measurements in close proximity to the critical point are necessary to develop an accurate model to cover the entire critical region, i.e., the extended critical region as well as the critical region proper. A thermal conductivity table has been prepared in terms of temperature (K) and pressure (bar). These tables are available from the authors.

ACKNOWLEDGMENTS

This work was performed under a program of studies funded by the Natural Sciences and Engineering Research Council, Canada, under Grant no. A8859.

NOMENCLATURE

a_k, b_{ij}, b_k, c_i	Parameters of regression model, $k = 0$ to n , $i = 0$ to m , $j = 0$ to n
P	Pressure, MPa (or bar)
Q_l	Heat flux per unit length, $\text{mW} \cdot \text{m}^{-1}$
t	Time, s
T	Temperature, K
T_{cr}	Critical temperature, K
T_r	Reduced temperature = T/T_{cr}
ΔT_w	Temperature rise of wire between time t_1 and t_2 , K
ΔT^*	Reduced temperature difference $(T - T_{cr})/T_{cr}$
λ	Thermal conductivity, $\text{mW} \cdot \text{m}^{-1} \cdot \text{K}^{-1}$
λ_1	Thermal conductivity at 1 bar, $\text{mW} \cdot \text{m}^{-1} \cdot \text{K}^{-1}$
λ_{bg}	Background thermal conductivity, $\text{mW} \cdot \text{m}^{-1} \cdot \text{K}^{-1}$
$\Delta\lambda_{cr}$	Thermal conductivity anomaly, $\text{mW} \cdot \text{m}^{-1} \cdot \text{K}^{-1}$
$\Delta\lambda_e$	Excess thermal conductivity, $\text{mW} \cdot \text{m}^{-1} \cdot \text{K}^{-1}$
ρ	Density, $\text{g} \cdot \text{cm}^{-3}$
ρ_{cr}	Critical density, $\text{g} \cdot \text{cm}^{-3}$
ρ_r	Reduced density, $=\rho/\rho_{cr}$
$\Delta\rho^*$	Reduced density difference $=(\rho - \rho_{cr})/\rho_{cr}$

APPENDIX

Table A1. Thermal Conductivity of Ethane: The Experimental Data

Ser. #	Test ID	T (K)	P (bar)	ρ ($\text{g} \cdot \text{cm}^{-3}$)	λ ($\text{mW} \cdot \text{m}^{-1} \cdot \text{K}^{-1}$)
1	ETH-01.010	293.85	14.45	0.0203	21.91
2	ETH-01.011	293.72	14.44	0.0203	22.16
3	ETH-01.012	293.59	14.44	0.0204	22.06
4	ETH-01.018	293.20	31.17	0.0575	25.63
5	ETH-01.261	297.16	189.78	0.4225	103.84
6	ETH-01.262	295.49	176.42	0.4210	101.47
7	ETH-01.263	295.39	200.48	0.4281	105.17
8	ETH-01.264	295.36	200.90	0.4282	105.43
9	ETH-01.265	295.36	251.30	0.4405	111.79
10	ETH-01.266	295.37	299.83	0.4504	116.75
11	ETH-01.267	294.17	37.83	0.0858	31.74
12	ETH-01.268	294.14	38.07	0.0871	33.12
13	ETH-01.269	294.25	44.82	0.3412	80.99
14	ETH-01.270	294.30	50.14	0.3516	82.08
15	ETH-01.271	294.34	50.19	0.3516	81.73
16	ETH-01.272	294.42	60.26	0.3641	83.84
17	ETH-01.273	294.51	70.33	0.3732	85.64

Table AI. (Continued)

Ser. #	Test ID	T (K)	P (bar)	ρ (g·cm ⁻³)	λ (mW·m ⁻¹ ·K ⁻¹)
18	ETH-01.274	294.61	80.18	0.3804	87.92
19	ETH-01.275	294.70	90.04	0.3866	89.63
20	ETH-01.276	294.81	101.11	0.3926	91.31
21	ETH-01.277	294.91	150.10	0.4133	98.30
22	ETH-01.278	294.51	188.81	0.4261	103.69
23	ETH-01.279	294.40	300.03	0.4516	117.21
24	ETH-01.280	294.35	350.01	0.4603	122.45
25	ETH-01.281	294.31	399.93	0.4681	126.65
26	ETH-01.282	294.25	450.12	0.4751	130.52
27	ETH-01.283	294.25	500.32	0.4814	136.25
28	ETH-01.284	294.24	550.37	0.4872	139.86
29	ETH-01.285	294.24	600.36	0.4926	143.73
30	ETH-01.286	294.25	650.14	0.4974	146.96
31	ETH-01.287	294.27	699.17	0.5021	150.64
32	ETH-01.288	293.15	6.90	0.0090	20.66
33	ETH-01.289	293.05	13.71	0.0192	21.68
34	ETH-01.290	293.14	20.70	0.0316	23.10
35	ETH-01.291	294.72	20.83	0.0315	22.67
36	ETH-01.292	294.72	20.84	0.0316	22.79
37	ETH-01.293	294.74	27.60	0.0464	24.44
38	ETH-01.294	294.82	34.57	0.0686	29.38
39	ETH-01.300	295.74	6.90	0.0089	21.41
40	ETH-01.301	295.84	13.79	0.0191	21.93
41	ETH-01.302	295.98	1.77	0.0022	20.54
42	ETH-01.224	318.03	599.28	0.4725	134.45
43	ETH-01.227	318.36	601.07	0.4725	133.72
44	ETH-01.228	318.44	651.40	0.4779	136.64
45	ETH-01.229	318.50	701.05	0.4834	139.77
46	ETH-01.230	318.68	552.67	0.4662	130.16
47	ETH-01.231	318.69	550.05	0.4659	129.80
48	ETH-01.332	318.71	550.05	0.4659	128.90
49	ETH-01.233	318.74	500.33	0.4591	124.93
50	ETH-01.234	318.76	450.69	0.4517	121.10
51	ETH-01.235	318.79	400.36	0.4434	116.38
52	ETH-01.236	318.98	349.67	0.4336	111.84
53	ETH-01.237	318.99	300.44	0.4229	106.62
54	ETH-01.238	319.01	250.17	0.4096	102.01
55	ETH-01.239	319.10	201.36	0.3935	95.90
56	ETH-01.240	319.26	150.54	0.3701	86.85
57	ETH-01.241	319.52	150.19	0.3695	87.15
58	ETH-01.249	315.57	39.36	0.0660	30.35
59	ETH-01.251	314.99	38.20	0.0632	29.82
60	ETH-01.252	314.99	49.95	0.1102	37.89
61	ETH-01.254	315.50	70.12	0.2814	72.09
62	ETH-01.255	315.58	82.02	0.3144	74.54

Table AI. (Continued)

Ser. #	Test ID	T (K)	P (bar)	ρ (g·cm ⁻³)	λ (mW·m ⁻¹ ·K ⁻¹)
63	ETH-01.256	315.69	80.68	0.3114	73.47
64	ETH-01.257	315.75	90.40	0.3278	75.48
65	ETH-01.258	315.86	100.53	0.3399	78.17
66	ETH-01.259	316.41	138.96	0.3689	86.70
67	ETH-01.260	316.55	201.01	0.3972	96.15
68	ETH-01.304	315.53	1.78	0.0021	23.07
69	ETH-01.305	316.13	3.45	0.0040	23.34
70	ETH-01.306	316.28	6.88	0.0082	23.74
71	ETH-01.307	316.40	13.78	0.0174	24.41
72	ETH-01.308	316.79	20.69	0.0275	25.77
73	ETH-01.309	316.88	27.57	0.0392	26.83
74	ETH-01.310	316.99	34.47	0.0531	28.62
75	ETH-01.311	317.14	40.66	0.0684	30.69
76	ETH-01.312	317.43	40.86	0.0687	30.64
77	ETH-01.313	314.63	37.52	0.0616	29.33
78	ETH-01.315	315.12	48.27	0.0997	37.52
79	ETH-01.320	316.47	51.73	0.1197	39.30
80	ETH-01.321	316.55	51.83	0.1202	39.27
81	ETH-01.322	316.62	51.97	0.1209	39.27
82	ETH-01.323	316.70	51.76	0.1189	39.76
83	ETH-01.324	318.68	57.21	0.1539	48.43
84	ETH-01.325	318.66	58.91	0.1678	52.65
85	ETH-01.326	318.64	62.23	0.1976	64.72
86	ETH-01.327	318.63	55.23	0.1388	43.08
87	ETH-01.328	318.65	51.79	0.1100	38.35
88	ETH-01.329	318.70	48.49	0.0930	35.13
89	ETH-01.330	318.74	44.90	0.0797	32.30
90	ETH-01.331	318.79	43.41	0.0749	31.87
91	ETH-01.332	318.82	71.22	0.2640	70.92
92	ETH-01.184	350.49	43.90	0.0582	33.69
93	ETH-01.185	350.33	48.23	0.0662	34.71
94	ETH-01.189	348.42	472.76	0.4274	111.57
95	ETH-01.194	349.53	350.17	0.4002	101.82
96	ETH-01.196	349.92	451.46	0.4222	111.22
97	ETH-01.197	350.78	456.15	0.4222	111.23
98	ETH-01.198	351.16	501.93	0.4301	113.72
99	ETH-01.199	351.28	549.91	0.4378	117.76
100	ETH-01.200	351.33	600.38	0.4452	122.01
101	ETH-01.202	350.60	100.64	0.2151	60.60
102	ETH-01.203	350.78	101.64	0.2172	60.28
103	ETH-01.204	350.90	150.55	0.3029	73.62
104	ETH-01.205	350.91	150.48	0.3028	74.10
105	ETH-01.206	350.98	200.19	0.3416	82.70
106	ETH-01.207	351.18	249.35	0.3655	89.64
107	ETH-01.208	349.17	229.56	0.3597	87.56

Table AI. (Continued)

Ser. #	Test ID	T (K)	P (bar)	ρ (g·cm ⁻³)	λ (mW·m ⁻¹ ·K ⁻¹)
108	ETH-01.209	349.03	250.73	0.3690	90.16
109	ETH-01.210	349.00	300.71	0.3868	96.06
110	ETH-01.211	348.99	353.19	0.4015	101.89
111	ETH-01.212	349.05	400.14	0.4126	106.41
112	ETH-01.213	349.07	70.19	0.1203	42.65
113	ETH-01.214	349.07	71.91	0.1258	43.35
114	ETH-01.215	349.16	61.51	0.0962	38.29
115	ETH-01.216	349.21	80.33	0.1535	48.62
116	ETH-01.217	349.31	90.32	0.1877	54.48
117	ETH-01.335	350.38	73.12	0.1270	43.46
118	ETH-01.338	351.15	687.79	0.4566	129.33
119	ETH-01.339	351.21	700.82	0.4583	130.58
120	ETH-01.345	349.87	3.44	0.0036	28.00
121	ETH-01.350	349.98	13.77	0.0152	28.97
122	ETH-01.351	349.99	20.70	0.0237	30.00
123	ETH-01.352	350.00	27.57	0.0329	30.88
124	ETH-01.353	350.01	34.49	0.0429	31.61
125	ETH-01.354	350.02	37.93	0.0483	32.14
126	ETH-01.355	350.05	41.38	0.0540	32.82
127	ETH-01.356	350.22	41.35	0.0539	32.87
128	ETH-01.357	350.14	44.82	0.0600	33.66
129	ETH-01.358	350.10	48.25	0.0663	34.39
130	ETH-01.359	350.09	51.75	0.0732	35.37
131	ETH-01.360	350.09	54.26	0.0784	36.30
132	ETH-01.361	350.08	54.22	0.0783	35.80
133	ETH-01.047	394.17	49.22	0.0534	39.64
134	ETH-01.048	395.90	49.80	0.0538	40.58
135	ETH-01.049	396.20	49.40	0.0532	40.81
136	ETH-01.050	396.42	50.27	0.0543	40.79
137	ETH-01.052	396.73	100.37	0.1303	48.56
138	ETH-01.059	397.75	149.82	0.2083	59.83
139	ETH-01.060	397.54	199.91	0.2651	69.11
140	ETH-01.064	398.33	299.89	0.3274	80.67
141	ETH-01.065	397.98	338.99	0.3436	84.47
142	ETH-01.066	397.75	338.36	0.3436	84.82
143	ETH-01.067	397.66	350.36	0.3482	86.25
144	ETH-01.068	397.67	450.61	0.3777	95.35
145	ETH-01.069	397.70	451.37	0.3778	95.68
146	ETH-01.070	397.75	500.39	0.3891	99.81
147	ETH-01.071	397.85	599.54	0.4081	107.47
148	ETH-01.072	397.87	700.14	0.4239	114.81
149	ETH-01.073	397.96	698.07	0.4235	113.77
150	ETH-01.074	397.96	402.08	0.3644	91.50
151	ETH-01.075	397.97	250.80	0.3020	76.38
152	ETH-01.076	397.98	200.82	0.2652	68.86

Table AI. (Continued)

Ser. #	Test ID	T (K)	P (bar)	ρ (g·cm ⁻³)	λ (mW·m ⁻¹ ·K ⁻¹)
153	ETH-01.077	397.80	150.18	0.2087	60.25
154	ETH-01.078	397.71	100.12	0.1289	48.71
155	ETH-01.362	398.21	47.32	0.0501	40.94
156	ETH-01.363	398.16	48.26	0.0513	40.03
157	ETH-01.364	398.35	44.92	0.0471	39.73
158	ETH-01.365	398.35	41.77	0.0434	39.30
159	ETH-01.366	398.36	41.43	0.0430	39.18
160	ETH-01.369	398.83	3.78	0.0035	35.78
161	ETH-01.370	398.88	6.88	0.0064	36.19
162	ETH-01.371	398.93	13.77	0.0130	36.74
163	ETH-01.372	398.99	20.66	0.0200	37.46
164	ETH-01.373	399.03	27.56	0.0273	37.91
165	ETH-01.374	399.07	34.46	0.0348	38.91
166	ETH-01.375	399.09	34.44	0.0348	39.12
167	ETH-01.376	398.08	51.46	0.0554	40.32
168	ETH-01.377	397.92	55.16	0.0602	41.01
169	ETH-01.378	397.89	62.06	0.0695	41.95
170	ETH-01.379	397.87	68.95	0.0793	43.05
171	ETH-01.079	500.66	41.00	0.0311	55.37
172	ETH-01.094	500.92	300.31	0.2304	77.82
173	ETH-01.095	500.30	351.48	0.2564	81.79
174	ETH-01.096	499.82	401.12	0.2777	87.13
175	ETH-01.099	498.59	600.17	0.3374	100.03
176	ETH-01.103	497.38	157.04	0.1315	65.50
177	ETH-01.105	497.08	100.29	0.0816	59.74
178	ETH-01.109	494.96	49.69	0.0385	56.30
179	ETH-01.110	495.72	450.06	0.2982	90.73
180	ETH-01.111	495.74	499.98	0.3136	94.67
181	ETH-01.112	495.79	499.56	0.3135	94.71
182	ETH-01.389	501.15	37.40	0.0282	55.17
183	ETH-01.393	500.40	651.25	0.3468	103.84
184	ETH-01.394	500.26	650.70	0.3468	104.07
185	ETH-01.395	499.93	602.65	0.3370	101.13
186	ETH-01.396	499.79	550.94	0.3248	97.41
187	ETH-01.397	497.37	495.37	0.3111	94.46
188	ETH-01.398	497.10	450.97	0.2975	90.93
189	ETH-01.399	497.08	401.19	0.2797	87.42
190	ETH-01.400	497.12	351.96	0.2589	83.42
191	ETH-01.401	497.17	301.49	0.2337	79.08
192	ETH-01.402	497.19	250.67	0.2032	74.28
193	ETH-01.403	497.42	199.99	0.1669	69.33
194	ETH-01.404	497.40	150.14	0.1255	65.16
195	ETH-01.405	497.48	102.22	0.0831	60.21
196	ETH-01.406	497.54	89.80	0.0723	59.25
197	ETH-01.407	497.59	70.59	0.0557	57.89

Table AI. (Continued)

Ser. #	Test ID	T (K)	P (bar)	ρ (g·cm ⁻³)	λ (mW·m ⁻¹ ·K ⁻¹)
198	ETH-01.408	498.11	62.41	0.0488	57.51
199	ETH-01.409	498.13	50.42	0.0389	56.32
200	ETH-01.410	498.20	51.07	0.0394	56.72
201	ETH-01.411	498.22	55.25	0.0428	57.13
202	ETH-01.412	498.22	55.46	0.0430	57.31
203	ETH-01.413	495.66	38.76	0.0297	55.71
204	ETH-01.414	495.61	40.86	0.0314	55.17
205	ETH-01.415	495.58	40.55	0.0311	55.42
206	ETH-01.416	495.54	48.85	0.0379	56.51
207	ETH-01.419	495.52	3.44	0.0025	54.09
208	ETH-01.420	495.53	6.89	0.0051	54.11
209	ETH-01.421	495.54	13.78	0.0102	54.35
210	ETH-01.422	495.55	20.67	0.0155	54.36
211	ETH-01.423	495.58	27.57	0.0208	55.08
212	ETH-01.424	495.60	34.46	0.0263	55.22
213	ETH-01.425	495.64	34.46	0.0263	55.20
214	ETH-01.120	600.27	345.55	0.1980	91.56
215	ETH-01.121	600.35	402.36	0.2209	95.14
216	ETH-01.122	600.23	400.77	0.2204	94.40
217	ETH-01.123	600.14	450.27	0.2382	97.64
218	ETH-01.127	599.76	497.63	0.2537	99.93
219	ETH-01.128	599.75	500.18	0.2545	99.70
220	ETH-01.129	599.75	549.75	0.2689	102.11
221	ETH-01.130	599.79	599.53	0.2820	105.18
222	ETH-01.131	599.76	629.94	0.2890	106.65
223	ETH-01.133	599.71	649.93	0.2936	107.60
224	ETH-01.134	599.63	500.39	0.2546	100.05
225	ETH-01.135	599.58	350.56	0.2005	92.25
226	ETH-01.136	599.56	250.28	0.1524	86.40
227	ETH-01.137	599.52	150.37	0.0942	80.63
228	ETH-01.138	599.49	100.01	0.0625	77.91
229	ETH-01.139	599.27	100.15	0.0626	78.06
230	ETH-01.140	599.32	149.93	0.0940	81.05
231	ETH-01.141	599.36	100.32	0.0627	77.77
323	ETH-01.144	599.45	39.74	0.0244	75.29
233	ETH-01.145	599.24	199.26	0.1239	83.53
234	ETH-01.439	597.77	68.14	0.0424	76.67
235	ETH-01.440	597.77	62.16	0.0386	76.45
236	ETH-01.441	597.77	55.35	0.0343	76.56
237	ETH-01.442	597.77	48.43	0.0299	76.22
238	ETH-01.443	597.84	41.33	0.0255	75.80
239	ETH-01.444	597.90	41.42	0.0255	76.08

REFERENCES

1. W. B. Mann and B. G. Dickins, *Proc. Roy. Soc. (London)* **A134**:77 (1931), and references therein.
2. Ye. Borovik, A. Matveyev, and Ye. Panina, *J. Tech. Phys. (USSR)* **10**:988 (1940).
3. H. Senftleben and H. Gladisch, *Z. Physik* **125**:653 (1949).
4. J. M. Lenoir, W. A. Junk, and E. W. Comings, *Chem. Eng. Progr.* **49**:539 (1955).
5. H. Senftleben, *Z. angew. Physik* **5**:33 (1953).
6. R. G. Vines and L. A. Bennett, *J. Chem. Phys.* **22**:260 (1954).
7. F. G. Keyes, *Trans. ASME*, 809-816 (July, 1954).
8. J. D. Lambert, K. J. Cotten, M. W. Pailthorpe, A. M. Robinson, J. Scrivins, W. R. F. Vale, and R. M. Young, *Proc. Roy. Soc. A231*:280 (1950).
9. D. E. Leng, E. M. Comings, *Ind. Eng. Chem.* **49**:2042 (1957).
10. V. H. Geier and K. Schafer, *Allg. Warmetechnik* **10**:70 (1961).
11. L. T. Carmichael, V. Berry, and B. H. Sage, *J. Chem. Eng. Data* **8**:281 (1965).
12. B. Le Neindre, R. Tufeu, P. Bury, P. Johannin, and B. Vodar, Experimental study of thermal conductivity of coefficients of methane and ethane between 25°C and 450°C at pressures up to 1000 bars. Laboratoire des Hautes Pressions-C.N.R.S., Bellevue, France (1969).
13. A. A. Clifford, E. Dickinson, and P. Gray, *J. Chem. Soc. (London)*, *Faraday Trans., Part I*, **72**:1997 (1976).
14. L. V. Yakush, N. A. Venicheva, and L. S. Saitseva, *J. Eng. Phys.* **37**:1071 (1979).
15. H. J. M. Hanley, K. E. Gubbins, and S. Murad, *J. Phys. Chem. Ref. Data* **16**:1167 (1977). Idem, private Communication, errata, July 1981.
16. R. C. Prasad and J. E. S. Venard, Idem, An apparatus to measure the thermal conductivity of fluids using the transient line source technique, to be published.
17. E. F. M. Van der Held and F. G. Van Drunen, *Physika* **15**:865 (1949).
18. N. Mani, Precise determination of the thermal conductivity of fluids using absolute transient hot-wire technique, Ph.D. dissertation, University of Calgary, Canada (1971).
19. J. V. Sengers, R. S. Basu, and J. M. H. Levelt Sengers, Representative equations for the thermodynamic and transport properties of fluids near the gas-liquid critical point, NASA Contractor Report 3424 (May 1981), p. 59.
20. N. W. Tsederberg, *Thermal Conductivity of Gases and Liquids* (M.I.T. Press, Cambridge, Mass., 1965).
21. B. Le Neindre, R. Tufeu, P. Bury, and J. B. Sengers, Berichte der Dunsen-Gesellschaft für physikalische Chemie **77**:262 (1973).
22. R. D. Goodwin, H. M. Roder, and G. C. Straty, Thermophysical properties of ethane from 90 to 600 K at pressures to 700 bars, Report No. NBS TN 684 (August 1976).
23. A. Michels, J. V. Sengers, and P. S. Vander Gulik, *Physica* **28** (1962).
24. A. M. Sirota, V. I. Latunin, and G. M. Belyaeva, *Teploenergetika* **21**:52 (1974).
25. H. M. Roder, *J. Res. Natl. Bur. Stand. (U.S.)* **87**:279 (1982).
26. R. C. Prasad, Measurement of the thermal conductivity of fluids, Ph.D. dissertation, Univ. of New Brunswick, Canada (1982).